Sarcomere dynamics and contraction-induced injury to maximally activated single muscle fibres from soleus muscles of rats

Peter C. D. Macpherson, Robert G. Dennis and John A. Faulkner*

Institute of Gerontology and Department of Physiology, University of Michigan, Ann Arbor, MI 48109-2007, USA

1. The focal nature of contraction-induced injury to skeletal muscle fibres may arise from heterogeneities in sarcomere length that develop during contractions. We tested the hypothesis that when a maximally activated single permeabilized fibre segment is stretched and a deficit in maximum isometric force (force deficit) is produced, the regions of sarcomeres with the longest lengths prior to the stretch contain the majority of the damaged sarcomeres when the fibre is returned to optimum length (L_o) after the stretch.

2. Single fibre segments ($n = 16$) were obtained from soleus muscles of rats. Average sarcomere length at five discrete positions along the length of each fibre was determined by lateral deflection of a diode laser spot. Diffraction patterns were obtained while fibres were relaxed and immediately before, during and after a single stretch of 40% strain relative to L_o. Following the stretch, the regions of each fibre that potentially contained damaged sarcomeres were identified by an increased scatter of the first-order diffraction patterns. The damage was confirmed by light and electron microscopy.

3. While single fibre segments were in relaxing solution, the mean value for all of the average sarcomere lengths sampled ($n = 80$) was 2·53 ± 0·01 μm (range, 2·40–2·68 μm). During the maximum isometric contraction before each stretch, the mean sarcomere length decreased to 2·42 ± 0·02 μm and the range increased to 2·12–3·01 μm.

4. During the stretch of 40% strain, all regions of sarcomeres were stretched onto the descending limb of the length–force curve, but sarcomere lengthening was non-uniform. After the stretch, when the maximally activated fibres were returned to L_o, the force deficit was 10 ± 1%. Microscopic evaluation confirmed that the regions with the longest sarcomere lengths before the stretch contained the majority of the damaged sarcomeres after the stretch. We conclude that when heterogeneities in sarcomere length develop in single permeabilized fibre segments during a maximum isometric contraction, the sarcomeres in the regions with the longest lengths are the most susceptible to contraction-induced injury.

During physical activities, skeletal muscle fibres can be injured by their own contractions. Such a contraction-induced injury is more likely to occur when muscles are stretched during contractions than when they shorten or remain at a fixed length (McCully & Faulkner, 1985). Focal damage to muscle fibres was evident by electron microscopy immediately following stretches of activated muscle groups (Fridén, Sjöström & Ekblom, 1983; Newham, McPhail, Mills & Edwards, 1983; Ogilvie, Armstrong, Baird & Bottoms, 1988), single whole muscles (Wood, Morgan & Proske, 1993; Brooks, Zerba & Faulkner, 1995), single intact fibres (Brown & Hill, 1991) and single permeabilized fibre segments (Macpherson, Schork & Faulkner, 1996). In each case, the focal damage observed was localized within single sarcomeres or small groups of sarcomeres which were in series and in parallel with intact sarcomeres. The initiation of injury during single stretches of contracting whole muscles (Brooks *et al.* 1995) and single permeabilized fibre segments (Macpherson *et al.* 1996) involves a combination of strain and the force developed during the stretch, but the mechanism responsible for the focal nature of contraction-induced injury has not been determined.

When skeletal muscles are stretched during a contraction, the initial increase in force is extremely rapid and then gives way to a more gradual rise in force over the remaining portion of the stretch. During the stretch, the transition from the rapid to the gradual rise in force has been defined as sarcomere 'yielding' (Flintney & Hirst, 1978). For a

* To whom correspondence should be addressed.

single sarcomere on the plateau or descending limb of the length–force relationship, an increase in force beyond the yield point cannot be explained by cross-bridge models of force generation (Harry, Ward, Heglund, Morgan & McMahon, 1990). Subsequently, Morgan (1990) demonstrated that a continued rise in force beyond the yield point could be modelled accurately only when heterogeneities in sarcomere length were incorporated into computer simulations. Furthermore, the model predicted that during a stretch, the longest, presumably weakest, sarcomeres individually undergo a loss of thick and thin filament overlap that results in rapid uncontrolled elongation, whereas shorter sarcomeres are strained but maintain filament overlap. Although heterogeneities in sarcomere length have been proposed to lead to the localized loss of thick and thin filament overlap and damage to small groups of sarcomeres during stretches of contracting muscle fibres (Newham *et al.* 1983; Morgan, 1990; Brown & Hill, 1991; Brooks *et al.* 1995; Macpherson *et al.* 1996), this hypothesis has not been supported by definitive evidence.

Our purpose was to determine the relationship between the heterogeneities in sarcomere length that develop during a maximum isometric contraction and the location of the injury following single stretches of maximally activated single permeabilized fibre segments obtained from soleus muscles of rats. Immediately before and after a stretch of 40% strain, the average sarcomere lengths of each of five discrete regions along the length of the individual fibres were determined by laser diffraction. We tested the hypothesis that when a maximally activated single permeabilized fibre segment is stretched and a deficit in maximum isometric force (force deficit) is produced, the regions of sarcomeres with the longest lengths prior to the stretch contain the majority of the damaged sarcomeres when the fibre is returned to optimum length (L_0) after the stretch. A brief report of these results was presented to the Biophysical Society (Macpherson & Faulkner, 1995).

METHODS

Data were collected on single permeabilized fibres ($n = 23$: experimental, 16; control, 7) from the soleus muscles ($n = 4$) of adult (5–6 months old) male rats. The rats were obtained from the specific pathogen-free colony of Sprague–Dawley rats raised in the barrier-protected Core Facility for Aged Rodents at the University of Michigan. All operations were conducted in compliance with the Guide for the Care and Use of Laboratory Animals (NIH publication no. 86-23).

Permeabilization of single fibre segments

Preliminary experiments performed on permeabilized fibre segments from extensor digitorum longus and soleus muscles of rats indicated that during maximum isometric activation, soleus fibre segments maintained greater uniformity of sarcomere length and produced first-order diffraction patterns with more distinct dominant peaks. Consequently, all experiments were performed on single permeabilized fibre segments from soleus muscles. To obtain soleus muscles, rats were anaesthetized with an intraperitoneal injection of sodium pentobarbitone (50 mg kg^{-1}) with supplemental doses administered as needed to prevent responses to tactile stimuli. The soleus muscles were exposed and the proximal and distal tendons were isolated. The tendons were cut and each soleus muscle was removed from the hindlimb. Soleus muscles were placed in cold (4 °C) buffered physiological salt solution (mM: 137 NaCl, 24 $NaHCO_3$, 11 glucose, 5 KCl, 2 $CaCl_2$, 1 $MgSO_4$, 1 NaH_2PO_4 and 0·025 tubocurarine chloride), which was maintained at a pH of approximately 7·4 with a gas mixture of 95% O_2 and 5% CO_2. After the soleus muscles were removed, the rats were killed with an overdose of sodium pentobarbitone.

Each muscle was cut longitudinally and transversely into bundles consisting of 50–100 fibre segments. The bundles of fibre segments were tied to glass capillary tubes with 5-0 suture with bundles lengthened until they were just taut. The bundles were then placed in ice-cold skinning solution. The skinning solution contained 50% (v/v) glycerol and relaxing solution (for composition see below). Fibres were stored in skinning solution at 4 °C for 24 h and then at −20 °C for up to 2 weeks.

Solutions

Relaxing and maximum activating solution contained (mM): 1 free Mg^{2+}, 4·4 total ATP, 7·0 EGTA, 20·0 imidazole, 14·5 creatine phosphate, and sufficient KCl to yield a total ionic strength of 180 mmol l^{-1}. Each solution was adjusted to pH 7·0 with KOH. Relaxing solution had a pCa of 9·0. The maximum activating solution had a pCa of 4·5. The final concentrations of each metal, ligand and metal–ligand complex for all experimental solutions were calculated with the use of the computer program of Fabiato & Fabiato (1979) and the stability constants listed by Godt & Lindley (1982). The apparent stability constant of Ca-EGTA ($2·39 \times 10^6$ M^{-1}) was corrected for ionic strength, pH and temperature. All experiments were performed at 15 ± 1 °C.

Measurement of contractile properties

For a given experiment, a bundle of fibres was removed from the skinning solution and placed in relaxing solution. With dark-field illumination of a dissecting microscope, single permeabilized fibre segments were pulled from the bundle with fine forceps. Single fibre segments were transferred to a chamber containing relaxing solution located in the baseplate of the apparatus used to measure contractile properties. One end of the fibre was laid in a trough made at the end of a 2 cm length of stainless-steel tubing (i.d., 180 μm). The tubing was attached to a capacitance–force transducer (model 400A; Cambridge Technology, Inc., Watertown, MA, USA). The other end of the fibre was placed in a trough at the end of a length of tubing that was attached to the lever arm of a servomotor (model 300; Cambridge Technology, Inc.). A nylon 5-0 monofilament plug was placed on the upper surface of each end of the fibre, and then the ends of the fibre and monofilament plugs were secured to the troughs with 10-0 suture ties (Metzger, Greaser & Moss, 1989). A microcomputer controlled the displacements of the lever arm of the servomotor and sampled forces measured by the force transducer.

Fibre segment length was set initially with the fibre just taut. Sarcomere length and fibre width were then measured using a stereomicroscope (M32; Wild-Heerbrugg), high power objective, and a camera system (MPS51S, MPS45; Wild-Heerbrugg). Sarcomere length and fibre width were determined from a Polaroid photomicrograph of the fibre (×400 magnification). Average sarcomere length (~2·2 to ~2·4 μm) was determined by measuring the length of 100 sarcomeres. Fibre depth was determined using a displacement micrometer by focusing (×400 magnification) initially on the upper surface of the fibre and then focusing on the bottom surface of the fibre. Surface to surface distance was defined as fibre depth. With the assumption of an elliptical cross-section, the

measurements of fibre depth and width were used to calculate the cross-sectional area of single fibres. We used the same experimental apparatus and procedures to measure the horizontal diameter of stainless-steel tubing while in relaxing solution and while in air and found no discernible difference. Consequently, the refractive index of the relaxing solution (1·33) was only taken into consideration for calculations of fibre depth. Based on the initial fibre segment length, the length of the fibre segment was adjusted to correspond to an average sarcomere length of 2·55 μm. Although we did not determine L_0 for each fibre, an average sarcomere length of 2·55 μm is within the range of sarcomere lengths required for the development of maximum isometric force (P_0) by permeabilized fibre segments from soleus muscles of rats (Stephenson & Williams, 1982). The specific P_0 (kN m^{-2}) for each fibre was determined by dividing the P_0 developed during an initial maximum calcium activation (pCa 4·5) by the CSA of the fibre. In the present study, the specific P_0 of $85 \pm 1{\cdot}5$ kN m^{-2} was similar to the value of $87 \pm 14{\cdot}0$ kN m^{-2} reported for permeabilized fibre segments from soleus muscles of rats (Metzger & Moss, 1990).

Measurement of average sarcomere length for five discrete regions

For single striated muscle fibres, measures of light diffraction have been validated as a method of determining average sarcomere lengths (Rüdel & Zite-Ferenczy, 1979; Roos & Leung, 1987). With the length of a given fibre segment adjusted to correspond to an average sarcomere length of 2·55 μm, the fibre was aligned directly in the path of the laser beam (Fig. 1). Fibre segments were transilluminated by a 4·2 mW linearly polarized diode laser (Applied Laser Systems; wavelength, 670 nm) with an elliptical beam. The laser was positioned such that the beam first passed through a 57 mm focal length meniscus lens, then a square 1 cm^3 quartz prism and finally through the optics of the microscope used to view the single fibre segments (Fig. 1). Single fibres were positioned perpendicular to the path of the laser beam with the long axis of the elliptical laser spot orthogonal to the length of the fibre. Coupled with the optics of the microscope, the 57 mm focal length meniscus lens focused the minor diameter of the elliptical laser beam to ~200 μm.

The square prism was used to deflect the laser beam laterally as shown in Fig. 1 (inset). By rotating the prism through 90 deg, the laser beam could be translated along the length of a fibre segment over a range of ~5 mm without changing the incident angle of the laser beam. A servomechanism was constructed to rotate the prism and a feedback controller was designed to allow any one of five preset prism angles to be achieved repeatedly. While single fibres were in relaxing solution, the prism was rotated by manual adjustment of potentiometers to position the laser beam so that it passed through five discrete points of approximately equal separation along the length of a given fibre segment (1·6–2·5 mm long). Electronically controlled positioning accuracy of the laser spot was within 50 μm. During experiments the hold time at each position was 500 ms and the maximum amount of time required to move between positions was ~300 ms. By automating the positioning of the laser spot, and with the laser beam diameter focused to ~200 μm, we were able to obtain five discrete diffraction patterns in less than 5 s. The five diffraction patterns represented 40–60% of the total number of sarcomeres in a given single fibre segment.

Diffraction patterns produced by each of the five regions of sarcomeres sampled along the length of a given fibre segment

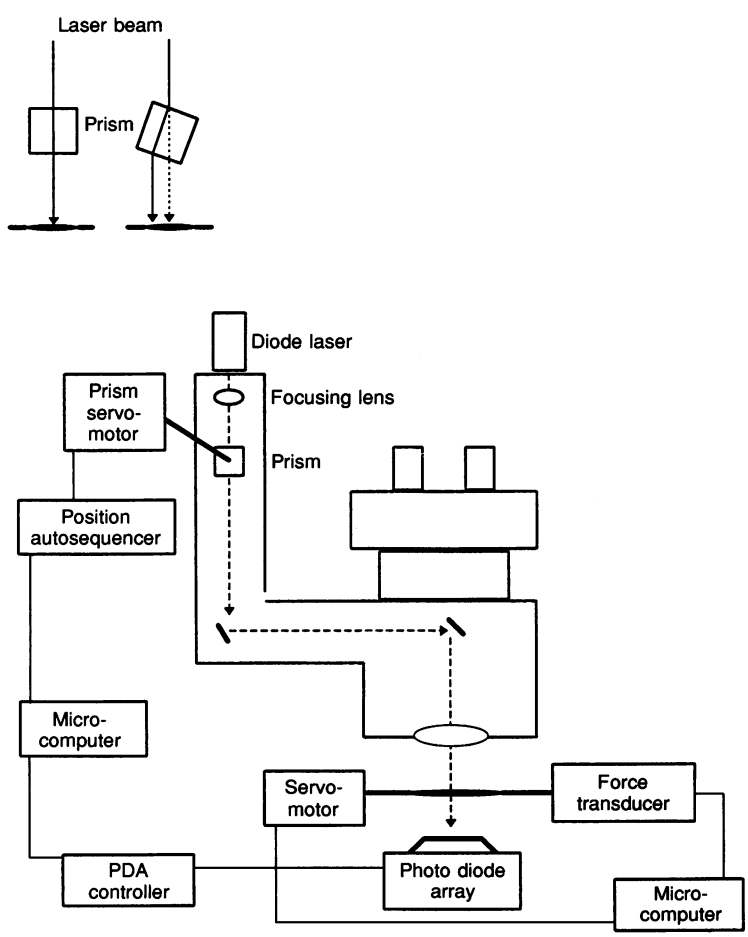

Figure 1. A schematic representation of the apparatus for measuring single muscle fibre contractile properties and obtaining diffraction patterns at multiple positions along the length of a single fibre segment

During maximum activation, in a pCa 4·5 solution, force measurements are obtained with a strain-gauge force transducer and isovelocity stretches are performed by a position feedback servomotor. A linear polarized diode laser is used to transilluminate a single fibre segment and determine the average sarcomere length at discrete positions along the length of the fibre. The beam path of the laser (see Methods) is denoted by the dashed line. The shape of the laser beam is elliptical and at the level of the single fibre segment the minor axis of the beam is focused to a diameter of ~200 μm. By rotating a square prism through 90 deg, the position of the laser beam is translated along the length of a single fibre segment (inset) with a maximum range of ~5 mm.

passed through a coverslip on the lower surface of the experimental chambers and were detected by a 2048 element photodiode array (RY-2048, Princeton Instruments, Inc., Trenton, NJ, USA). The intensity of the zeroth-order pattern was reduced with neutral-density filters to make it comparable to the intensity of the first-order pattern. Diffraction data were collected by a photodiode array controller (ST-121, Princeton Instruments, Inc.) and subsequently analysed with a microcomputer running software designed for the analysis of diode array output (CSMA software, Princeton Instruments, Inc.). Sampling time for each diffraction pattern was 50 ms, and to ensure internal consistency four patterns were obtained each time a region of sarcomeres was sampled. Average sarcomere length was calculated according to the diffraction grating equation using the distance measured between the centre of the zeroth order and the maximum of the dominant peak of the left first-order diffraction pattern.

Protocol for the induction of injury

For maximally activated permeabilized fibre segments from soleus muscles of rats, single stretches of 40% strain relative to L_0 at 0·5 fibre lengths s^{-1} were required to produce a 10% force deficit that was associated with damage to the ultrastructure of sarcomeres (Macpherson *et al.* 1996). In the present study, each single stretch was initiated following the development of P_0 and each stretch was through a strain of 40%. Strain was defined as the change in length relative to the fibre segment length at L_0. The velocity of stretch was 0·5 fibre lengths s^{-1}. Immediately following the stretch the fibre was returned to L_0 at the same velocity.

At the beginning of each experiment ($n = 10$), diffraction patterns were obtained at each of the five positions while the fibre was in relaxing solution. The fibre was then transferred to maximum activating solution (pCa 4·5), developed P_0, and diffraction patterns were obtained for each of the same regions of sarcomeres. The fibre was returned to the relaxing solution and the diffraction patterns that were obtained during the period of maximum activation were viewed to ensure that dominant peaks were present in each of the first-order patterns during the initial period of maximum activation. Following the initial assessment of first-order diffraction patterns, the fibre was transferred back into maximum activating solution to obtain a second set of diffraction patterns during an isometric contraction. Immediately after obtaining this second set, the fibre was stretched (Fig. 2*A*). Following the return to L_0 and redevelopment of isometric force at L_0 (Fig. 2*B*), a third set of diffraction patterns was obtained. The fibre was then returned to relaxing solution and subsequently processed for morphological evaluation or discarded.

Six additional single fibre segments were studied to assess sarcomere dynamics during a single stretch of 40% strain. In contrast to the previous experiments, the fibre was stretched to 140% of L_0 and then held at this length. Due to the 40% increase in fibre length, diffraction patterns were obtained from six regions of sarcomeres rather than five. By manually triggering the position feedback controller of the prism servomotor we were able to obtain the sixth diffraction pattern with an additional delay time of ~3 s.

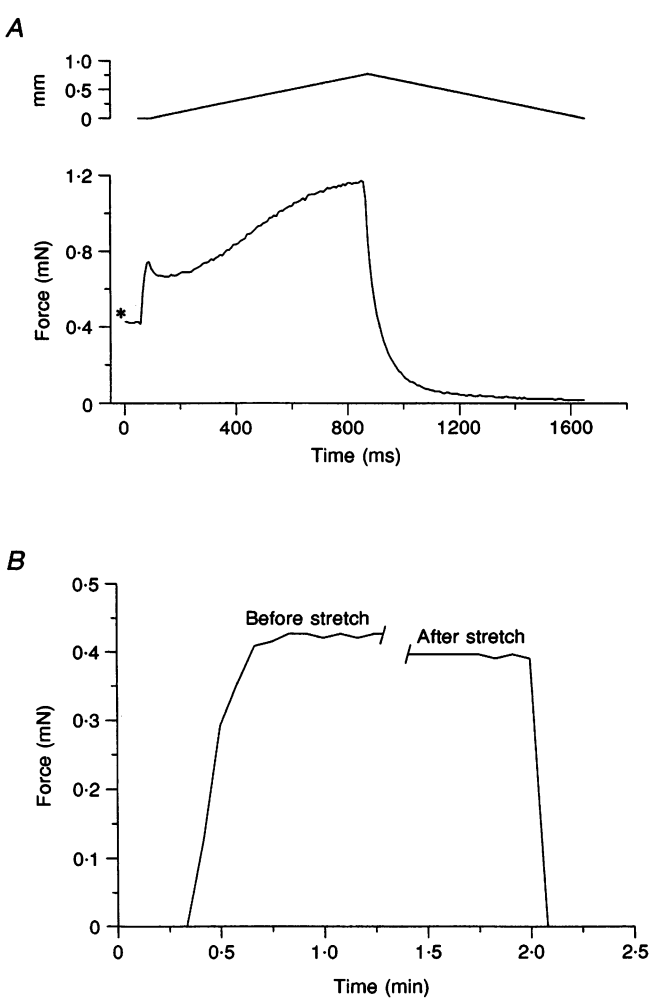

Figure 2. Representative force and isometric force traces in a single fibre before, during and after a single stretch of 40% strain at 0·5 fibre lengths s^{-1}

A, representative force trace of a maximally activated single fibre during a single stretch of 40% strain at 0·5 fibre lengths s^{-1}. The upper trace is the displacement applied to a fibre by the servomotor measured in millimetres from L_0. The lower trace is the corresponding force response during the stretch. The asterisk (*) indicates the maximum isometric force before the stretch. *B*, the maximum isometric force developed before and after the single stretch of 40% strain. Single fibres were not removed from the maximum activating solution until a post-stretch P_0 was obtained. The difference between the pre-stretch P_0 and the post-stretch P_0 was defined as the force deficit. Note: the force response during the stretch is on a different time scale from the isometric force values and is not present in *B*.

Tissue fixation for light and electron microscopy

For eight of the fibres that were exposed to a stretch of 40% strain and then immediately returned to L_o, the location of the damage to sarcomeres was identified with light microscopy. For five of these fibres, damage to the ultrastructure of specific regions of sarcomeres was assessed with electron microscopy. Following post-stretch measurements of P_o, fibres were returned to relaxing solution and then placed into fixative within 30 s of relaxation. The methods used for tissue fixation and embedding have been described previously (Macpherson *et al.* 1996). Longitudinal semi-thick sections (1 μm thick), or ultrathin sections (50 nm thick), were cut with a diamond knife mounted on an ultramicrotome (MT 5000; Sorvall). Semi-thick sections were mounted on glass microscope slides and stained with a 1% (w/v) Toluidine Blue solution. Ultrathin sections were mounted on uncoated copper grids and stained with aqueous uranyl acetate and lead citrate. Light microscopic evaluation of the overall morphology of fibre segments was performed on semi-thick sections with an oil-immersion lens (×100 magnification). Ultrathin sections were examined with a transmission electron microscope (CM-10; Philips) at 60 kV to assess damage to the ultrastructure of sarcomeres.

Statistical analysis

Values are presented as means ± 1 S.E.M. Differences between specific P_o values (kN m^{-2}), obtained before and after the stretch, were evaluated by a one-tailed paired t test. To determine differences in average sarcomere length during maximum activation before the stretch, average sarcomere lengths were arranged according to length, from shortest to longest for each fibre, and then the means were assessed by a univariate one-way analysis of variance (ANOVA). If the F statistic of the ANOVA showed significance, differences were determined by pairwise t tests and adjusted for multiple comparisons (Bonferroni). The level of significance was set *a priori* at $P < 0.05$.

RESULTS

Frequency distributions of the average sarcomere lengths were constructed from the diffraction patterns of each of the regions of sarcomeres sampled while single fibres were in relaxing solution and during maximum activation just prior to the stretch. For relaxed fibres ($n = 16$), the mean sarcomere length for all of the regions of sarcomeres sampled ($n = 80$) was 2·53 ± 0·01 μm with a range of 2·40–2·68 μm (Fig. 3). For maximally activated fibres immediately before the stretch the mean sarcomere length was 2·42 ± 0·02 μm and the variability in average sarcomere length increased with a range of 2·12–3·01 μm (Fig. 3). Consistent with the results of Julian & Moss (1980), in ~70% of the passive single permeabilized fibre segments we observed that the sarcomeres at the longer lengths were not the regions of sarcomeres with the longest lengths during the maximum isometric contractions. In only 25% of the fibres were the sarcomeres at the longer lengths in passive fibres stretched following activation.

The initial drop in force during the period of stretch (Fig. 2*A*) appears to be a characteristic of slow muscle fibres (Stienen, Versteeg, Papp & Elzinga, 1992). During an earlier series of experiments in which maximally activated single fibre segments from fast and slow muscles were stretched over a variety of strains from 5 to 40% (Macpherson *et al.* 1996), we consistently observed the initial drop in force for slow fibres, but not for fast fibres. To further test whether the initial drop in force during the period of stretch (Fig. 2*A*) was due to fibre slippage, carbon markers were placed on the extreme ends of five fibres and then marker movement was monitored visually and with light photomicrographs (×400 magnification) during maximum activation immediately before, during and after an imposed stretch of 40% strain. During the development of maximum isometric force, marker separation decreased by ~3·0 ± 1% of initial fibre segment length. A decrease in marker separation of 3% was in good agreement with the decrease in sarcomere length of 5 ± 1% (from 2·53 to 2·42 μm) which occurred during the development of maximum isometric force. When the fibres were returned to relaxing solution after the stretch, marker spacing was reduced by 2·0 ± 0·5% of initial fibre segment length. These data indicated that at least 1% of the shortening during the isometric contraction before the stretch was reversible even after a 40% stretch. During the period

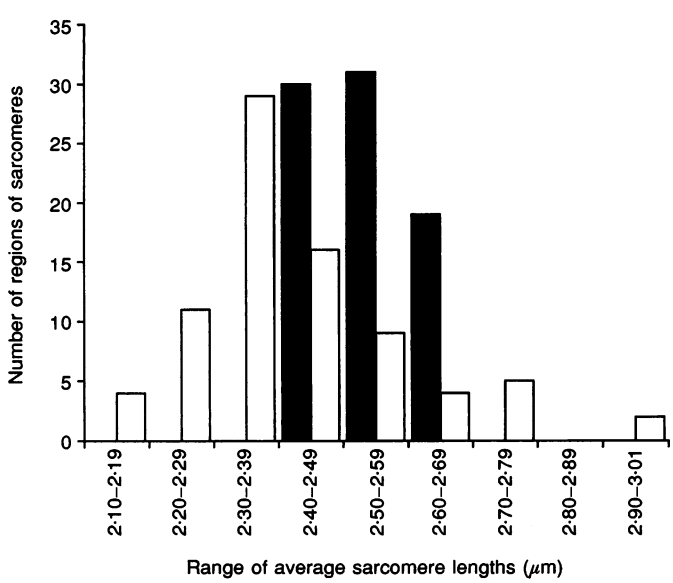

Figure 3. Frequency distribution of average sarcomere lengths of single fibre segments ($n = 16$) from soleus muscle of rats obtained while in relaxing solution (■) and during a maximally activated isometric contraction just prior to a stretch of 40% strain (□)

Diffraction patterns of each of five discrete regions along the length of a single fibre segment were obtained by transilluminating the given fibre segment with a diode laser. The average sarcomere length of each region ($n = 80$) was determined from the distance between zeroth-order and first-order diffraction peaks. With the laser beam diameter focused to ~200 μm, the five regions of sarcomeres sampled along the length of the single fibres (1·6–2·5 mm long) represented 40–60% of the total number of sarcomeres present in a given fibre segment.

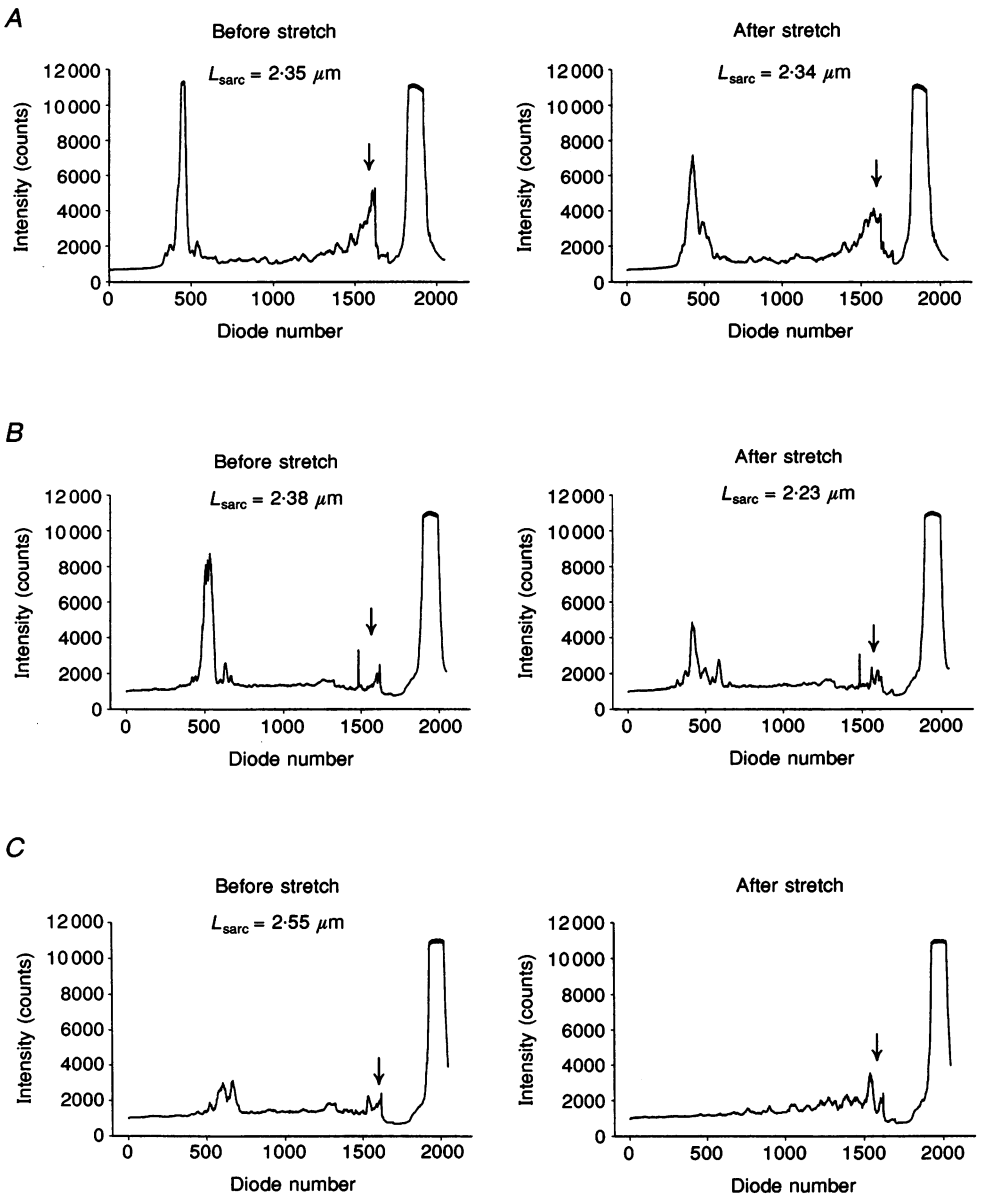

Figure 4. Representative zeroth- and first-order diffraction patterns obtained during maximum activation just before (left-hand side) and following a single stretch (right-hand side)

In each panel, the zeroth-order diffraction pattern is at the right of each frame. The arrow next to the zeroth peak indicates artifact caused by neutral-density filters used to reduce the intensity of the zeroth-order diffraction pattern. Abscissa labels are diode numbers and the estimated average sarcomere length determined from the corresponding diffraction pattern. The ordinate labels are the measured light intensity in counts (3800 photons per count) of the diffraction pattern. *A* contains diffraction patterns representative of all five regions of a control fibre which following a stretch of 30% strain showed no force deficit. For each of the five regions of sarcomeres sampled, average sarcomere lengths (L_{sarc}) changed by less than 2%. *B* and *C* present diffraction patterns representative of two different regions of the same (experimental) fibre which following a single stretch of 40% strain, showed a force defict of 12%. For eight out of ten fibres, as represented in *B*, the four regions of sarcomeres with the shortest sarcomere lengths during the isometric contraction immediately before the stretch (left) produced dominant peaks in each of the respective first-order diffraction patterns after the stretch (right). For the two other fibres, only three regions of sarcomeres with shorter lengths produced dominant first-order peaks following the stretch (as in *B*). In contrast, as shown in *C*, the regions of each fibre with the longest average sarcomere length prior to the stretch produced diffraction patterns that contained no dominant first-order peak.

of stretch, no overt indication of fibre slippage was observed and measurements of carbon marker separation during maximum activation, before and after the stretch, confirmed that fibre slippage at the points of attachment was negligible. Compared with marker separation before the stretch, after the stretch, marking separation relative to fibre length decreased by 0·16 ± 0·50%.

For the six fibres that were maximally activated, stretched with a 40% strain, and then held at the stretched length, a dominant peak was present in each of the first-order diffraction patterns obtained from the six regions of sarcomeres sampled. During the hold at 40% strain, the range of average sarcomere lengths obtained from the different regions of the fibres was 3·01–3·76 μm. These data demonstrated that the lengthening of sarcomeres occurred non-uniformly and that by the end of the stretch of 40% strain, each of the regions of sarcomeres sampled was on the descending limb of the length–force relationship. Despite the magnitude of the stretch, none of the regions displayed an average sarcomere length greater than 3·95 μm, which would have been consistent with the loss of thick and thin filament overlap (Woledge, Curtin & Homsher, 1985). Following the accumulation of diffraction patterns and return to L_0, the maximum isometric forces developed by these fibres were unstable and during a subsequent maximum activation the fibres began to tear apart. Consequently, force deficit measures and morphological evaluations were not performed on these fibres.

Two control experiments were conducted on maximally activated fibre segments that were exposed to a single isovelocity stretch of either 10 or 30% strain to evaluate the stability of the diffraction pattern following return to L_0. In each of these two cases, no force deficit was produced following the stretch. The diffraction patterns and corresponding average sarcomere lengths of the five regions of sarcomeres sampled following each of these stretches were not significantly different from those obtained immediately before the stretch (Fig. 4*A*).

Following a single stretch of 40% strain and immediate return to L_0, a significant force deficit was produced in each of the ten maximally activated single fibre segments. The mean force deficit was 10 ± 1%. For eight of the ten fibres, when fibres were returned to L_0, the four regions of each fibre with the shorter average sarcomere lengths prior to the stretch displayed dominant peaks in the first-order diffraction patterns (Fig. 4*B*). In contrast, the region of each fibre with the longest average sarcomere length prior to the stretch produced a severely attenuated first-order diffraction pattern that contained no dominant peak following the stretch (Fig. 4*C*). For two of the fibres, two regions displayed attenuated peaks in the first-order diffraction patterns after the stretch. In each case, the two regions that lacked dominant peaks in the first-order diffraction patterns were adjacent to each other and one of each of the adjacent regions had developed the longest average sarcomere length before the stretch.

With the regions grouped according to rank based on the average sarcomere length during the isometric contraction before the stretch, the mean sarcomere lengths of the four shortest groups were not different. In contrast, the mean sarcomere length of the longest group was significantly longer than each of the other four groups (Fig. 5). After the stretch and return to L_0, average sarcomere length decreased in 60% of the fifty regions of sarcomeres

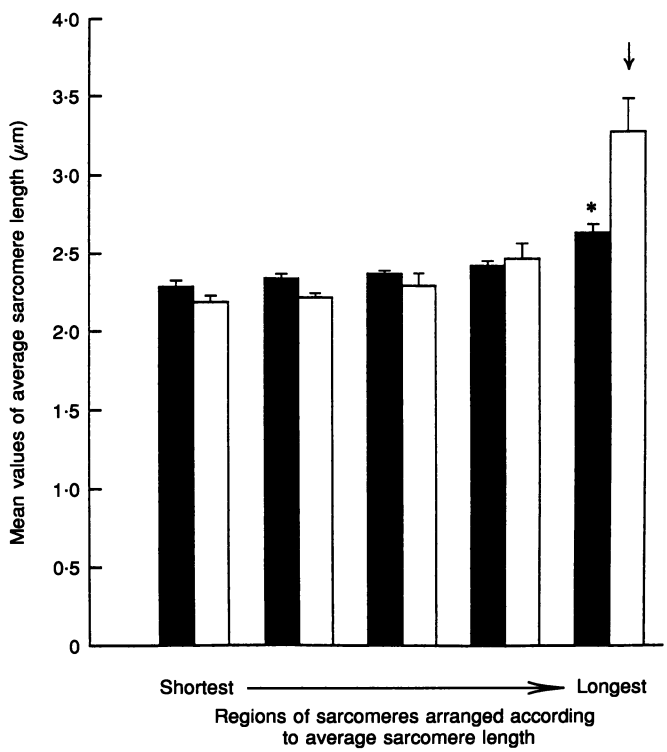

Figure 5. Mean values of average sarcomere length of each of five discrete regions of sarcomeres along the length of single fibres ($n = 10$) obtained during maximum activation just prior to (■) and immediately following a single stretch of 40% strain (□)

For each fibre, regions of sarcomeres were arranged according to average sarcomere length prior to the stretch such that region 1 represents the mean value obtained for the regions of sarcomeres with the shortest lengths ($n = 10$) and region 5 represents the mean value obtained for the regions of sarcomeres with the longest lengths ($n = 10$). Values given are means ± 1 S.E.M. Prior to the stretch, the mean value for the regions with the longest lengths (*) was significantly different from the mean values for the other regions ($P < 0·05$). Since following the stretch of 40% strain, the regions of sarcomeres with the longest average length prior to a stretch produced no dominant peaks in the first-order diffraction patterns, a mean value of average sarcomere length (3·28 ± 0·21 μm) was predicted for the region (arrow) based on the sarcomere length changes that occurred in other regions of the fibre.

sampled, 8% showed no change in length, 8% increased in length, and in 24% of the regions an average sarcomere length could not be calculated directly due to loss of a dominant peak in the first-order diffraction pattern. With the regions of sarcomeres grouped according to relative length before the stretch, the mean sarcomere length of the three shortest groups decreased by ~5% after the stretch (Fig. 5). For the next shortest group, the mean sarcomere length increased only slightly after the stretch (Fig. 5).

Average sarcomere lengths for each of the regions of sarcomeres that lacked first-order diffraction peaks after the stretch were estimated by dividing the total length of a given fibre segment by 5, and assuming each of the regions of sarcomeres sampled reflected the average sarcomere length for a 20% section of the fibre. Dividing the section lengths by the corresponding average sarcomere lengths obtained during maximum activation before the stretch provided an estimate of the number of sarcomeres present in each section. Subtracting the number of sarcomeres

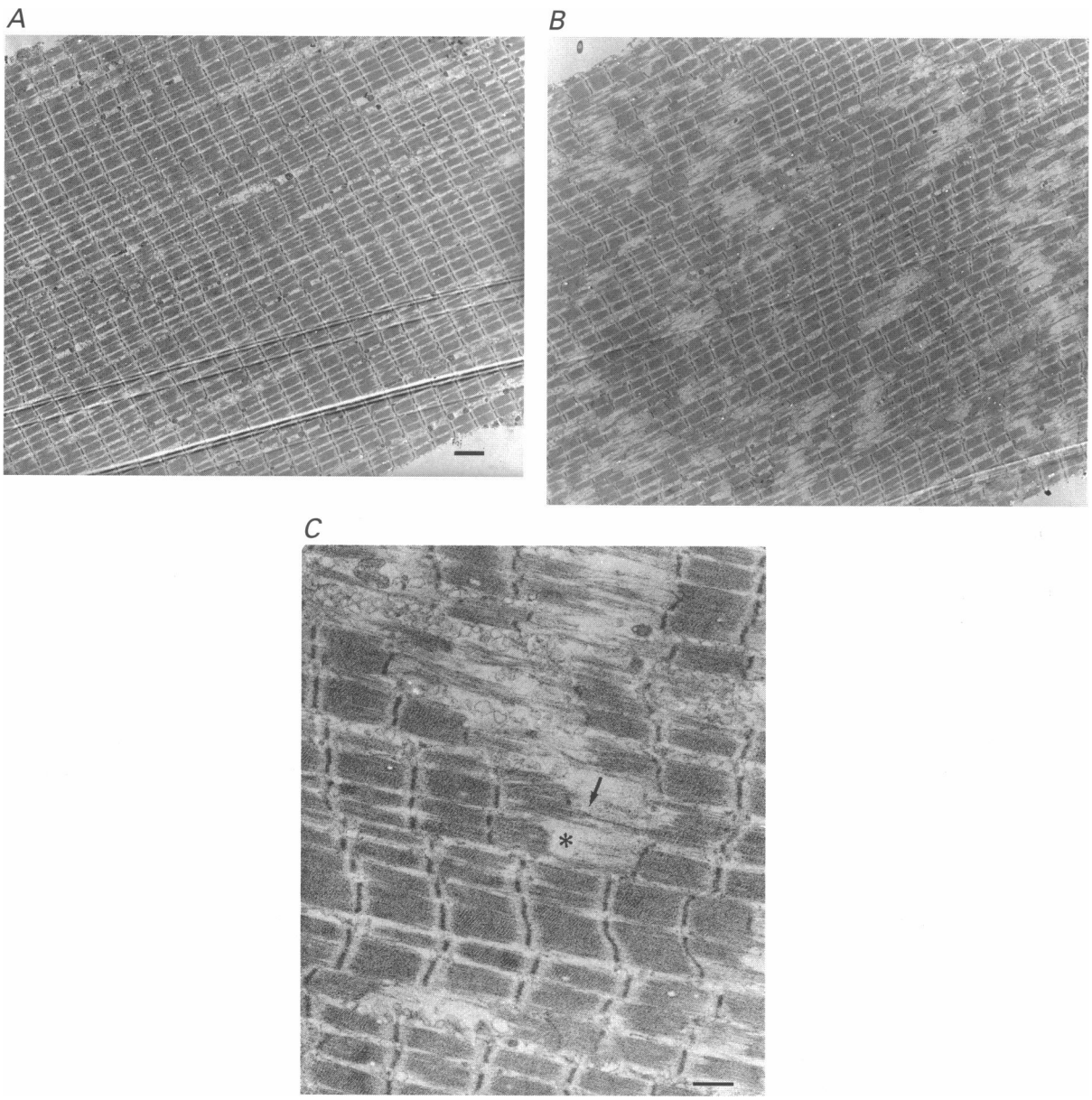

Figure 6. Electron micrographs of a relaxed single fibre following a single stretch of 40% during maximum activation

A, a longitudinal section of the fibre in which sarcomeres appear to be intact and not damaged. *B*, an adjacent region of the same fibre in which small groups of damage sarcomeres are in series and in parallel with intact sarcomeres. For *A* and *B* the magnification is ×4290. *C*, the same region of the fibre as in *B*, at a higher magnification (×17160). Damage to the ultrastructure of sarcomeres appears as loss of thick and thin filament interdigitation (*), streaming of Z-lines (arrow) and a loss of contractile material. Scale bars: 3·0 μm for *A* and *B*; 1·0 μm for *C*.

accounted for after the stretch from the total number of sarcomeres provided an estimate of the number of sarcomeres present in the regions of the fibre that lacked first-order diffraction peaks after the stretch. Average sarcomere lengths were predicted for each of these regions by dividing the section length of the region by the estimated number of sarcomeres present in the section.

For each of the regions with the longest sarcomere lengths prior to the stretch the indirect estimates of average sarcomere length predicted an increase in length after the stretch of approximately 25% (Fig. 5). In nine out of ten fibres, the region with the longest average sarcomere length before the stretch was at one end of the fibre. For each of the ten fibres, the region with the second longest average sarcomere length prior to the stretch was either adjacent to the region with the longest average sarcomere length, or in the middle of the fibre, but never at the opposite end of the fibre.

For the single fibres that were maximally activated, stretched, and returned immediately to L_0, light microscopic evaluation of fibre morphology indicated disruption and damage to sarcomeres in the same region as was indicated by the loss in the first-order diffraction patterns. Electron micrographs showed damage localized to individual sarcomeres or to small groups of sarcomeres in series and in parallel with intact undamaged sarcomeres (Fig. 6*A* and *B*). Damage to the ultrastructure of sarcomeres included loss of thick and thin filament interdigitation, streaming and disruption of Z-lines, and loss of sarcomere organization (Fig. 6*C*). Since light diffraction by sarcomeres requires ordered structure, the focal nature of the damage to small groups of sarcomeres and the loss of sarcomere organization caused by the damage provide an explanation as to why average sarcomere lengths consistent with loss of thick and thin filament overlap were neither observed when fibres were stretched and held at the longer length, nor when maximally activated fibres were returned to L_0.

DISCUSSION

The exact mechanism by which a given stretch causes localized damage to sarcomeres is unknown, but the focal nature of the damage suggests that the physical or functional properties of specific sarcomeres play a major role in the initiation of the injury. Hill (1949) was the first to the propose that during a maximum isometric tetanic contraction, weaker regions of a fibre shorten the least and stronger regions the most. Abbott & Aubert (1952) expanded this concept to include stretches of maximally activated fibres and postulated that weaker regions were stretched more than stronger regions. Experimental observations showed that when muscle fibres were stretched beyond L_0 and then maximally activated, the variability in sarcomere lengths increased significantly (Julian & Morgan, 1979*a*; Lieber & Baskin, 1983; Burton, Zagotta & Baskin, 1989). Furthermore, even during short single stretches of activated fibres, the lengthening of sarcomeres appeared to be non-uniform (Julian & Morgan, 1979*b*; Lombardi & Piazzesi, 1990). Morgan's (1990) computer model of the force response during single stretches of a maximally activated fibre predicted that the stretch resulted in a rapid uncontrolled lengthening, or 'pulling apart', of individual sarcomeres as single sarcomeres were stretched beyond overlap of thick and thin filaments. Our results support the concept of weaker sarcomeres being pulled apart, since with a single stretch, sarcomeres appear to lengthen in a highly non-uniform manner and after the stretch, the majority of damage was contained within the regions that developed the longest sarcomere length before the stretch.

If injury occurred before individual sarcomeres were stretched beyond thick and thin filament overlap, the mechanism of the injury would require either damage to cycling cross-bridges, or localized failure of passive elements, or a combination of these two factors. The limit to which a single cross-bridge can be stretched is between 10 and 15 nm (Flintney & Hirst, 1978; Lombardi & Piazzesi, 1990). For a sarcomere at L_0, this represents a strain of less than 1%. For maximally activated whole EDL muscles from mice (Brooks *et al.* 1995) and for single fibre segments from soleus muscles of rats (Macpherson *et al.* 1996), muscle fibres were stretched by a strain of 10% without subsequent development of a force deficit. These data indicate that contracting muscle fibres can be stretched by at least an order of magnitude beyond the maximum working distance of cycling cross-bridges without inducing a force deficit. Furthermore, when muscle fibres are stretched during a contraction, the rate constants for detachment and re-attachment of cross-bridges increase dramatically (Lombardi & Piazzesi, 1990). Thus forced detachment and recycling of cross-bridges appear to occur without damage to the cross-bridges.

Following single stretches of passive muscle fibres, despite the presence of some heterogeneity in sarcomere length initially, significant force deficits were not produced until fibres were stretched to lengths consistent with a loss of thick and thin filament overlap for all sarcomeres (Higuchi, Yoshioka & Maruyama, 1988; Brooks *et al.* 1995; Macpherson *et al.* 1996). In addition, Wang, McCarter, Wright, Beverly & Ramirez-Mitchell (1993) showed that damage to passive elements, such as titin and intermediate filaments, did not occur until passive fibre segments were stretched to lengths at which thick and thin filaments no longer overlapped. These observations suggest that localized failure of passive elements and damage to sarcomeres require strains that stretch sarcomeres beyond the overlap of thick and thin filaments.

In single intact fibres, the regions of sarcomeres with the shortest lengths are usually at the ends of the fibre (Huxley & Peachey, 1961; Gordon, Huxley & Julian, 1966). Our results and those of Julian & Moss (1980) show that for permeabilized fibres, the regions of sarcomeres that lengthen during maximum isometric contractions tend to be

at one end of the fibre segments. The difference in the distribution of sarcomere lengths between permeabilized fibre segments and intact fibres may be explained by the permeabilized fibre segment representing only a portion of the intact fibre which is usually obtained from an end of the intact fibre, to avoid the neuromuscular junction. Alternatively, the tendency for the sarcomeres with the longest lengths to be at one end of the fibre segments could have been due to the fibre attachment to the experimental apparatus weakening the sarcomeres adjacent to the attachment. This explanation seems unlikely since for each fibre segment, the region that developed the longest average sarcomere length was independent of location with respect to the force transducer or servomotor end of the fibre, and the region that developed the second longest length was never at the opposite end of the fibre. Furthermore, given the similarity of the method of fibre attachment at each end of the fibre, weakening of sarcomeres adjacent to only one of the fibre attachments is difficult to reconcile. If the fibre attachments weakened the sarcomeres adjacent to the attachment sites then sarcomeres at both ends of the fibre should have lengthened not only after the stretch, but during the maximum isometric contraction before the stretch. In 80% of the fibres evaluated, sarcomeres adjacent to the attachment at one end of the fibre shortened during the maximum isometric force before the stretch and/or shortened during the contraction after the stretch.

Although the phenomenon of contraction-induced injury was first described by Hough (1902) almost 100 years ago, the mechanism responsible for the immediate mechanical injury has proved elusive. For maximally activated whole muscles (Brooks *et al.* 1995) and single permeabilized fibres (Macpherson *et al.* 1996), the mechanical factors associated with the force deficit immediately following a single stretch involve a complex interaction of peak force, average force and strain. Electron micrographs obtained immediately after contraction protocols that result in the development of contraction-induced injury show evidence of focal damage to the ultrastructure of single sarcomeres (Fridén *et al.* 1983; Newham *et al.* 1983; Brown & Hill, 1991; Wood *et al.* 1993; Brooks *et al.* 1995; Macpherson *et al.* 1996). In conclusion, the totality of the current evidence from active and passive whole muscles, single intact fibres, single fibre segments, and computer simulations is consistent with the hypothesis that the initiating event in the development of contraction-induced injury occurs when longer sarcomeres in series with shorter sarcomeres are stretched excessively. Upon return to L_o, some of the sarcomeres at longer lengths are damaged and lose some portion of their ability to develop force.

Abbott, B. C. & Aubert, X. M. (1952). The force exerted by active striated muscle during and after changes of length. *Journal of Physiology* **117**, 77–86.

Brooks, S. V., Zerba, E. & Faulkner, J. A. (1995). Injury to muscle fibres after single stretches of passive and maximally stimulated muscles in mice. *Journal of Physiology* **488**, 459–469.

Brown, L. M. & Hill, L. (1991). Some observations on variations in filament overlap in tetanized muscle fibres and fibres stretched during a tetanus, detected in the electron microscope after rapid fixation. *Journal of Muscle Research and Cell Motility* **12**, 171–182.

Burton, K., Zagotta, W. N. & Baskin, R. J. (1989). Sarcomere length behaviour along single frog muscle fibres at different lengths during isometric tetani. *Journal of Muscle Research and Cell Motility* **10**, 67–84.

Fabiato, A. & Fabiato, F. (1979). Calculator programs for computing the composition of solutions containing multiple metals and ligands used for experiments in skinned muscle cells. *Journal de Physiologie* **75**, 463–505.

Flintney, F. W. & Hirst, D. G. (1978). Cross-bridge detachment and sarcomere 'give' during stretch of active frog's muscle. *Journal of Physiology* **276**, 449–465.

Fridén, J., Sjöström, M. & Ekblom, B. (1983). Myofibrillar damage following intense eccentric exercise in man. *International Journal of Sports Medicine* **4**, 170–176.

Godt, R. E. & Lindey, B. D. (1982). Influence of temperature upon contractile activation and isometric force production in mechanically skinned muscle fibres of the frog. *Journal of General Physiology* **80**, 279–297.

Gordon, A. M., Huxley, A. F. & Julian, F. J. (1966). Tension development in highly stretched vertebrate muscle fibres. *Journal of Physiology* **184**, 143–169.

Harry, J. D., Ward, A. W., Heglund, N. C., Morgan, D. L. & McMahon, T. A. (1990). Cross-bridge cycling theories cannot explain high-speed lengthening behavior in frog muscle. *Biophysical Journal* **57**, 201–208.

Higuchi, H., Yoshioka, T. & Marauyama, K. (1988). Positioning of actin filaments and tension generation in skinned muscle fibres released after stretch beyond overlap of actin and myosin filaments. *Journal of Muscle Research and Cell Motility* **9**, 491–498.

Hill, A. V. (1949). The energetics of relaxation in a muscle twitch. *Proceedings of the Royal Society of London* B **136**, 211–219.

Hough, T. (1902). Ergographic studies in muscular soreness. *American Journal of Physiology* **7**, 76–92

Huxley, A. F. & Peachey, L. D. (1961). The maximum length for contraction in vertebrate striated muscle. *Journal of Physiology* **156**, 150–165.

Julian, F. J. & Morgan, D. L. (1979*a*). Intersarcomere dynamics during fixed-end tetanic contractions of frog muscle fibres. *Journal of Physiology* **293**, 365–378.

Julian, F. J. & Morgan, D. L. (1979*b*). The effect of tension of non-uniform distribution of length changes applied to frog muscle fibres. *Journal of Physiology* **293**, 379–392.

Julian, F. J. & Moss, R. L. (1980). Sarcomere length–tension relations of frog skinned muscle fibres at lengths above the optimum. *Journal of Physiology* **304**, 529–539.

Lieber, R. L. & Baskin, R. J. (1983). Intersarcomere dynamics of single muscle fibers during fixed-tetani. *Journal of General Physiology* **82**, 347–364.

Lombardi, V. & Piazzesi, G. (1990). The contractile response during steady lengthening of stimulated frog fibres. *Journal of Physiology* **431**, 141–171.

McCully, K. K. & Faulkner, J. A. (1985). Injury to skeletal muscle fibres of mice following lengthening contractions. *Journal of Applied Physiology* **59**, 119–126.

Macpherson, P. C. D. & Faulkner, J. A. (1995). Sarcomere dynamics and contraction-induced injury to active single muscle fibres. *Biophysical Journal* **68**, A74.

Macpherson, P. C. D., Schork, M. A. & Faulkner, J. A. (1996). Contraction-induced injury to single fiber segments from fast and slow muscles of rats by single stretches. *American Journal of Physiology* **271**, C1438–1446.

Metzger, J. M., Greaser, M. L. & Moss, R. L. (1989). Variations in cross-bridge attachment rate and tension with phosphorylation of myosin in mammalian skinned skeletal muscle fibers: implications for twitch potentiation in intact muscle. *Journal of General Physiology* **93**, 855–883.

Metzger, J. M. & Moss, R. L. (1990). Effects of tension and stiffness due to reduced pH in mammalian fast- and slow-twitch skinned skeletal muscle fibres. *Journal of Physiology* **428**, 737–750.

Morgan, D. L. (1990). New insights into the behavior of muscle during active lengthening. *Biophysical Journal* **57**, 209–221.

Newham, D. J., McPhail, G., Mills, K. R. & Edwards, R. H. T. (1983). Ultrastructural changes after concentric and eccentric contractions of human muscle. *Journal of the Neurological Sciences* **61**, 109–122.

Ogilvie, R. W., Armstrong, R. B., Baird, K. E. & Bottoms, C. L. (1988). Lesions in the rat soleus muscle following eccentrically biased exercise. *American Journal of Anatomy* **182**, 335–346.

Roos, K. P. & Leung, A. L. (1987). Theoretical Fraunhofer light diffraction patterns calculated from three-dimensional sarcomere arrays imaged from isolated cardiac cells at rest. *Biophysical Journal* **52**, 329–341.

Rüdel, R. & Zite-Ferenczy, F. (1979). Interpretation of light diffraction by cross-striated muscle as Bragg reflexion of light by the lattice of contractile proteins. *Journal of Physiology* **290**, 317–330.

Stephenson, D. G. & Williams, D. A. (1982). Effects of sarcomere length on the force–pCa relation in fast- and slow-twitch skinned muscle fibres from the rat. *Journal of Physiology* **333**, 637–653.

Stienen, G. J. M., Versteeg, P. G. A., Papp, P. & Elzinga, G. (1992). Mechanical properties of skinned rabbit psoas and soleus muscle fibres during lengthening: effect of phosphate and Ca^{2+}. *Journal of Physiology* **451**, 503–523.

Wang, K., McCarter, R., Wright, J., Beverly, J. & Ramirez-Mitchell, R. (1993). Viscoelasticity of the sarcomere matrix of skeletal muscles: the titin–myosin composite filament is a dual-stage molecular spring. *Biophysical Journal* **64**, 1161–1177.

Woledge, R. C., Curtin, N. A. & Homsher, E. (1985). *Energetic Aspects of Muscle Contraction*, pp. 27–117. Academic Press Ltd, London.

Wood, S. A., Morgan, D. L. & Proske, U. (1993). Effects of repeated eccentric contractions on the structure and mechanical properties of toad sartorius muscle. *American Journal of Physiology* **265**, C792–800.

Acknowledgements

The authors thank Krystyna Pasyk for her preparation of the tissue for light and electron microscopic evaluation. This research was supported by a National Institute on Aging Grant, AG-06157.

Author's email address

J. A. Faulkner: jafaulk@umich.edu

Received 19 August 1996; accepted 15 January 1997.